



# Removal of cadmium (II) from aqueous solution by a new adsorbent of fluor-hydroxyapatite composites



Xin-hua Zhu, Jun Li\*, Jian-hong Luo\*, Yang Jin, Dan Zheng

College of Chemical Engineering, Sichuan University, Chengdu 610065, PR China

## ARTICLE INFO

### Article history:

Received 29 May 2016

Revised 5 September 2016

Accepted 24 October 2016

Available online 10 November 2016

### Keywords:

Fluorine-contained silica

Fluor-hydroxyapatite composites

Cadmium (II)

Adsorption

Desorption

## ABSTRACT

The excellent precursor of fluor-hydroxyapatite composites (FHA) was prepared by hydrothermal method using fluorine-contained silica (F-SiO<sub>2</sub>) and hydrated lime (HL) as raw materials. And a new adsorbent FHA was obtained and employed as an adsorbent for the removal of Cd<sup>2+</sup> from aqueous solution. Series of adsorption properties of FHA for the removal of Cd<sup>2+</sup> from aqueous solution were investigated at various conditions. The influence of different adsorption parameters, such as solution pH, initial concentration of Cd<sup>2+</sup>, temperature and contact time on the adsorption efficiencies of FHA for Cd<sup>2+</sup> were studied and discussed. The results showed that the adsorption process was in agreement with the Langmuir isotherm model and pseudo-second-order kinetic model. The Langmuir adsorption isotherm constant corresponding to adsorption amount,  $q_m$ , was found to be 236.41 mg/g. Various thermodynamic parameters such as  $\Delta G^0$ ,  $\Delta H^0$  and  $\Delta S^0$  were calculated, which indicated the spontaneous and endothermic nature of the adsorption process. At the appropriate conditions, FHA was an excellent adsorbent for the removal of Cd<sup>2+</sup> from aqueous solution. And it was confirmed that the adsorption mechanism of Cd<sup>2+</sup> by FHA was mainly determined by ion-exchange and monolayer chemical adsorption.

© 2016 Published by Elsevier B.V. on behalf of Taiwan Institute of Chemical Engineers.

## 1. Introduction

The effluents containing cadmium are produced in industries including metal plating, batteries, plastic, pigments, nonferrous mining and smelting, etc., [1,2] which migrating into water sources and farmlands pose a serious threat to plants, animals and even human beings because of the bioaccumulation, irreversibility and toxicity of cadmium ion. Thus, scholars have paid much attention for the removal and recovery of cadmium, and various methods such as chemical precipitation [3], reduction-oxidation [4], ion-exchange [5], forward osmosis [6], biological process [7] have been introduced for the removal of cadmium from aqueous solution. Among the different methods described above, adsorption process is attractive due to its merits of efficiency, economy and simple operation, and lots of studies on this process have been carried out [8–10].

Hydroxyapatite (Ca<sub>10</sub>(PO<sub>4</sub>)<sub>6</sub>(OH)<sub>2</sub>, HA) work as a novel environmentally functionalized ideal material because of its special

crystal structure, high stability, low water solubility, availability and low cost, has shown excellent ions adsorbability and exchangeability [11–14], which is characterized with high-efficiency adsorption amount for most of heavy metals in water, such as Cd<sup>2+</sup> [15], Cu<sup>2+</sup> [16], Zn<sup>2+</sup>, Pb<sup>2+</sup>, Co<sup>2+</sup> [17], Cr<sup>6+</sup> [18], Cr<sup>3+</sup>, Ni<sup>2+</sup> [19], Fe<sup>3+</sup> [20], As<sup>5+</sup> [21], etc.

At present, the silica containing 10% soluble fluoride is a solid waste discharged from the fluorine factory on a large scale. There are no effective management approaches to the dispose of fluorine-contained silica (F-SiO<sub>2</sub>), so the released fluoride may cause severe ecological and environment issues [22]. In this work, the authors try to introduce fluorine into HA to improve the adsorption performance of FHA for metal ions, because the diameter of fluorine ion is less than hydroxyl and the lattice of FHA is more compact [23]. And a little of fluorine is embedded in FHA, which cannot decrease permeability in a large degree because of the high specific surface area of FHA. In contrast, FHA with a compact structure can improve the adsorbent stability slightly. It may be a useful approach to deal with the F-SiO<sub>2</sub> by converting it into the adsorbent FHA. Furthermore, a systematic study of parameters such as solution pH, initial concentration of Cd<sup>2+</sup>, temperature and contact time were carried out in order to elucidate the adsorption behavior of Cd<sup>2+</sup> onto FHA as well as the desorption of Cd<sup>2+</sup> from this material by different eluents.

\* Corresponding authors.

E-mail addresses: [lijun@scu.edu.cn](mailto:lijun@scu.edu.cn) (J. Li), [luojianhong@scu.edu.cn](mailto:luojianhong@scu.edu.cn) (J.-h. Luo).

## 2. Materials and methods

### 2.1. Materials

Fluorine-contained silica (F-SiO<sub>2</sub>) with the amount of fluoride approximately 10% and 8.1 m<sup>2</sup>/g specific surface area was obtained from a fluorine plant of Yunnan in China. Hydrated lime (HL), Potassium dihydrogen phosphate (KH<sub>2</sub>PO<sub>4</sub>) and cadmium metal powder were purchased from Chengdu Kelong Chemical Co. Ltd. (China). Deionized water was produced by Aquapro making water machine (ABZ1-1001-P) in laboratory.

### 2.2. Preparation of precursor and FHA

Precursor was prepared as follows: F-SiO<sub>2</sub> and HL were mixed together with different Ca/Si molar ratio. The mixture was stirred for the formation of suspension in proper water/solid mass ratio, and transferred to a PTEE-lined hydrothermal reactor heated at different temperatures for 8 h. Then the precursor was obtained after filtering, washing, and drying at 105 °C for 6 h.

FHA composites were prepared as the following methods: At 25 °C and pH of 9.0, the precursor was slowly added to KH<sub>2</sub>PO<sub>4</sub> solution and stirred for 10 h. Then FHA composites were obtained after filtering, washing, and drying at 105 °C for 6 h.

### 2.3. Parameters that could affect the adsorption process

Stock solutions of Cd<sup>2+</sup> (1000 mg/l) were prepared by dissolving appropriate amount of the cadmium powder in HCl solution (0.06 mol/l) and HNO<sub>3</sub> solution (7.2 mmol/l). Working solutions ranging from 10 to 60 mg/l of Cd<sup>2+</sup> were prepared by diluting the stock solutions.

In order to study Cd<sup>2+</sup> removal efficiencies and advantages of the adsorption process, various parameters such as the kind of precursor, solution pH, initial Cd<sup>2+</sup> concentration, solution temperature and contact time that could affect the process must be optimized.

### 2.4. Desorption experiments

In order to estimate the reversibility of Cd<sup>2+</sup> adsorption, desorption studies were carried out. Adsorbents (0.1 g) loaded with Cd<sup>2+</sup> were regenerated in 50 ml of eluents (HCA, Ca(NO<sub>3</sub>)<sub>2</sub>, EDTA-2Na and NaOH) on a rotary shaker at 130 r/min and 25 °C for 10 h, the concentration of Cd<sup>2+</sup> in the eluents were measured to investigated the desorption efficiency.

### 2.5. Analysis

Brunauer–Emmett–Teller (BET) surface area of samples was measured from N<sub>2</sub> adsorption isotherms by homemade adsorption instrument according to Chinese national standard (GB/T 19,587-2004). Surface morphology and internal structure of samples were observed by S-4800 scanning electron microscope (Hitachi, Japan). Elemental composition of samples was analyzed by energy dispersive spectrometer (Hitachi, Japan).

The concentration of Cd<sup>2+</sup> was detected by dithizone spectrophotometry method (GB 7471–87) with the ultraviolet spectrophotometer (UV-1100) [24,25]. The lowest detectable concentration for Cd<sup>2+</sup> of this method was 0.001 mg/l and the linear equation of standard curve ( $Y = 3.8571X - 0.0004$ , the correlation coefficient of 0.9991) was obtained in the experiment. Adsorption amount of cadmium ( $q_e$ , mg/g) loaded in FHA after adsorption experiments and the removal percentage (Removal %) of Cd<sup>2+</sup> in aqueous solution could be calculated using the following

equations.

$$q_e = \frac{(C_0 - C_e) \times V}{m} \quad (1)$$

$$\text{Removal (\%)} = \frac{C_0 - C_e}{C_0} \times 100\% \quad (2)$$

Where  $C_e$  (mg/l) is the equilibrium cadmium concentration in solution,  $C_0$  (mg/l) is the initial cadmium concentration,  $m$  (g) is the mass of adsorbent, and  $V$  (L) is the volume of the solution.

## 3. Results and discussion

### 3.1. Characterization of precursor and FHA

Precursor, fluorine-contained calcium silicate, was prepared using F-SiO<sub>2</sub> and HL with different Ca/Si molar ratio (0.4, 0.7 and 0.9), temperature (120, 140 and 160 °C) and reaction time (8 h), the relationship between the specific surface area and experiment conditions of precursor was shown in Table 1. The precursor with high specific surface area was benefit to the formation of FHA with higher specific surface area and better adsorbability for Cd<sup>2+</sup>. When the Ca/Si molar ratio and temperature remained unchanged, the specific surface area of precursor increased with increasing the reaction time from 6 to 8 h. However, there was no significant change in the specific surface area when the reaction time was extended to 10 h. So reaction time of 8 h was chosen to preparation of precursor in all experiments. According to Table 1, the molar ratio of Ca/Si was the most significant effect on the specific surface area of precursor and the hydrothermal temperature was also an important influence factor. The reason could be explained that the precursor structure changes with the variation of Ca/Si molar ratio and temperature, which had been discussed in the previous work [26]. And a developed space connected mesh structure was obtained with the Ca/Si molar ratio of 0.7 and temperature of 120–140 °C, which was beneficial to formation of the precursor with high specific surface area. Therefore, the optimized parameters affecting the process were as follows: molar ratio of Ca/Si was 0.7, hydrothermal temperature was maintained from 120 to 140 °C, and reaction time was 8 h.

Three samples of FHA were indexed as A, B and C in the production of precursor by changing the temperatures from 120, 140 and 160 °C with Ca/Si molar ratio of 0.7 and reaction time of 8 h. Another two samples of FHA were indexed as D and E in the production of precursor by changing the Ca/Si molar ratio from 0.4 and 0.9 with temperature of 140 °C and reaction time of 8 h.

The results plotted in Fig. 1 clearly showing that samples B and D had significant adsorption amount and removal percentage for the removal of Cd<sup>2+</sup>. This was might be explained that the higher specific surface area of samples B and D (128.4 and 119.5 m<sup>2</sup>/g) shown in Fig. 2 than others provided more adsorption and ion-exchange sites, which improved the adsorbability of adsorbents. Judging from the SEM images showed in Fig. 2, it could also be confirmed that precursors with high specific surface area conducted to the formation of FHA with rod-like and developed space connected structure. Therefore, the samples B was chosen for adsorption in this study and used for further adsorption experiments.

### 3.2. Effect of pH

Solution pH was adjusted by NaOH (1.0 mol/l) and HCl (1.0 mol/l). The pH value in the range of 2.0–8.0 was chosen based on the reason that Cd<sup>2+</sup> started to precipitate when the pH was higher than 8.0 [14,27]. The relationship between solution pH and Cd<sup>2+</sup> adsorption amount was presented in Fig. 3. It was found that the adsorption amount of FHA for Cd<sup>2+</sup> was highly dependent

**Table 1**  
Relationship between preparation conditions and the specific surface area of precursor.

Samples	Ca/Si molar ratio	Temperature (°C)	Reaction time (h)	Surface area (m <sup>2</sup> /g)
1	0.4	120	6	65.25
2	0.4	120	10	80.12
3	0.4	120	8	79.30
4	0.7	140	8	122.50
5	0.9	160	8	69.87
6	0.4	140	8	55.27
7	0.7	120	8	143.80
8	0.9	140	8	52.85
9	0.4	160	8	43.25
10	0.7	160	8	106.40
11	0.9	120	8	79.22

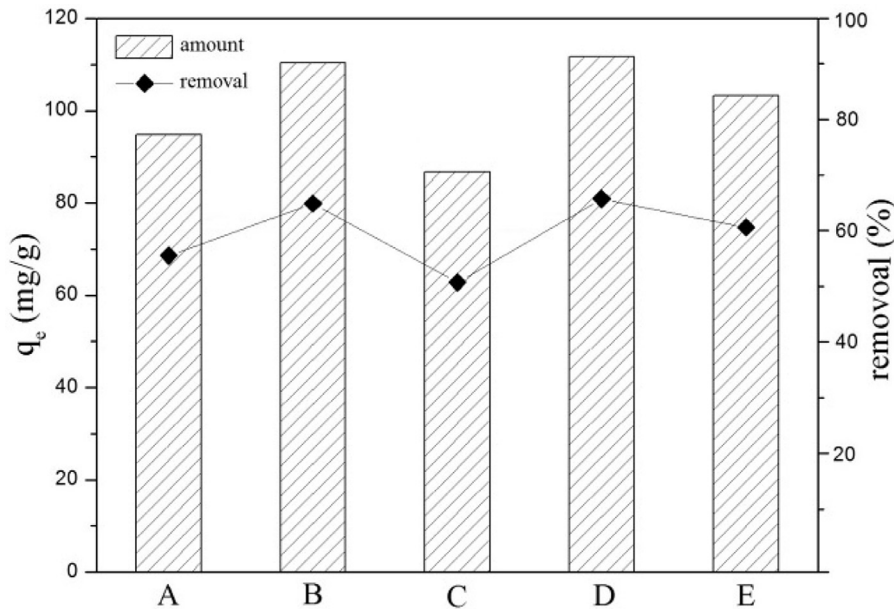


**Fig. 1.** The adsorption effects of FHA for Cd<sup>2+</sup>. Amount of adsorbent FHA, 0.3 g/l; initial Cd<sup>2+</sup> concentration, 50 mg/l; agitation speed, 130 r/min; solution pH, 5.0; adsorption time, 10 h; solution temperature, 25 °C.

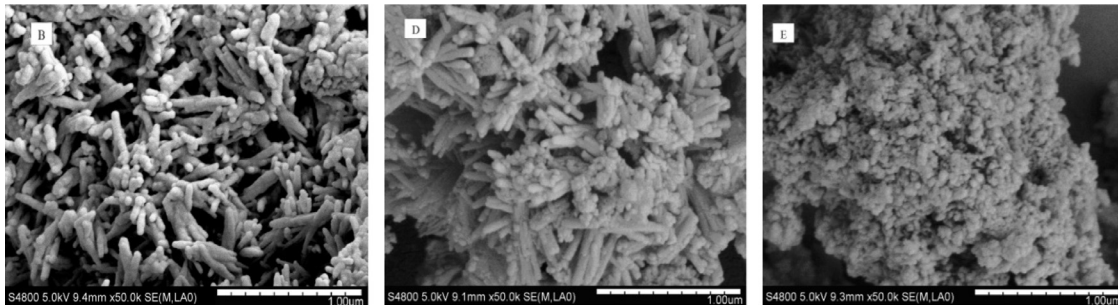


**Fig. 2.** SEM images of samples (B, D and E).

on pH, which was attributed to the fact that solution pH affected the solubility of metal ions and ionization state of the functional groups presented on the adsorbents [28].

Wu et al. [29] mentioned that the surface groups ( $\equiv\text{Ca}-\text{OH}_2^+$  and  $\equiv\text{P}-\text{O}^-$ ) of HA were highly depended on protonation and deprotonation by  $\text{H}^+$  and  $\text{OH}^-$  in aqueous solution, therefore, the surface groups changed with the difference in pH value. Furthermore, the positively charged  $\equiv\text{Ca}-\text{OH}_2^+$  and neutral  $\equiv\text{P}-\text{OH}$  sites prevailed on FHA surface in acidic solutions making surface charge of FHA positive, whereas neutral  $\equiv\text{Ca}-\text{OH}$  and negatively charged  $\equiv\text{P}-\text{O}^-$  species predominated in alkaline solutions causing FHA surface to become negative. On the other hand, in the pH range

from 2.0 to 8.0, cadmium was mainly in the form of  $\text{Cd}^{2+}$  in aqueous solution. As the pH value increased, the number of negatively charged active sites also increased resulting in an increase in adsorption amount [28]. This is because the electrostatic attraction increased with the increasing pH value.

It was well known that  $\text{Ca}^{2+}$  in HA could be easily ion-exchanged with many other metal ions [30]. The peak of cadmium appeared in the EDS spectra (Fig. 4) indicating FHA loaded with  $\text{Cd}^{2+}$ , furthermore, the calcium atomic ratio decreased sharply after FHA loading with  $\text{Cd}^{2+}$  according to Table 2. Combing with Fig. 4 and Table 2, it was concluded that this phenomenon was due to the ion-exchange mechanism on the adsorption of FHA for  $\text{Cd}^{2+}$ .

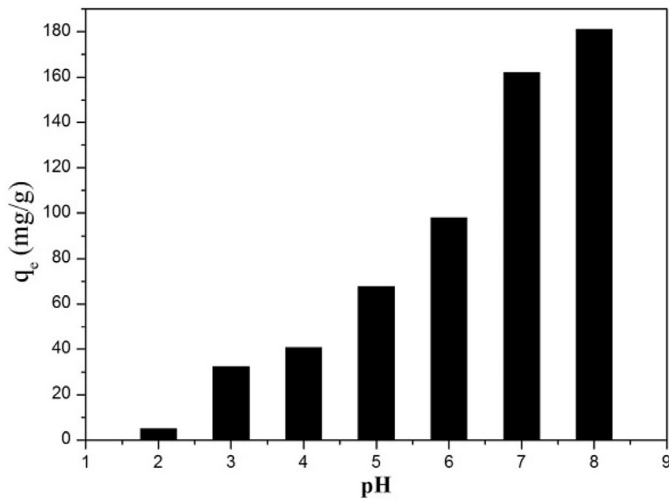


**Fig. 3.** The effect of solution pH on the adsorption of  $\text{Cd}^{2+}$  onto FHA. Amount of adsorbent FHA, 0.3 g/l; initial  $\text{Cd}^{2+}$  concentration, 60 mg/l; agitation speed, 130 r/min; adsorption time, 10 h; solution temperature, 25 °C.

**Table 2**

EDS analysis: elemental composition of FHA before and after  $\text{Cd}^{2+}$  adsorption.

Elements	Before adsorption		After adsorption	
	Weight (%)	Atomic (%)	Weight (%)	Atomic (%)
Oxygen	46.18	63.94	49.66	68.53
Fluorine	3.16	3.69	2.95	3.44
Silicon	9.56	7.54	10.41	8.42
Phosphorus	13.02	9.31	11.06	7.93
Calcium	28.08	15.52	18.37	9.73
Cadmium	–	–	7.55	1.89

Based on Fig. 3, the tremendous change of adsorption amount (5.11–181.19 mg/g) with the pH range of 2.0–8.0 suggested the adsorption mechanism should be the ion-exchange and the electrostatic during the adsorption process. Moreover, the optimum pH value for  $\text{Cd}^{2+}$  adsorption was found to be in the range of 7.0–8.0. And the pH range of 5.0–8.0 could be used in the real process of  $\text{Cd}^{2+}$  adsorption, because there were a good adsorption amount in the pH range of 5.0–8.0 and the real process usually worked under weak acidic conditions.

### 3.3. Effect of initial $\text{Cd}^{2+}$ concentration and adsorption isotherms

The effect of initial  $\text{Cd}^{2+}$  concentration on the adsorption of  $\text{Cd}^{2+}$  was shown in Fig. 5. It indicated that the amount of  $\text{Cd}^{2+}$  adsorbed onto FHA increased as the initial  $\text{Cd}^{2+}$  concentration increased. However, the tendency of  $\text{Cd}^{2+}$  adsorption amount increased steadily in the initial concentration up to 30 mg/l and then increased slowly. The reason for this phenomenon was that a certain amount of FHA provided enough adsorption sites with lower initial  $\text{Cd}^{2+}$  concentration before the maximum (conditions of saturation), and when the initial  $\text{Cd}^{2+}$  concentration was elevated, large numbers of  $\text{Cd}^{2+}$  competitively adsorbed on the same adsorption sites provided by FHA beyond the maximum resulting in the reduction of adsorption rate per unit adsorbent. In addition, it was found that the removal efficiencies of  $\text{Cd}^{2+}$  were more than 81% in different initial concentrations, especially those at the initial concentrations of 30 mg/l closed to 98%. Therefore, it was expected that FHA was an excellent adsorbent for the removal of  $\text{Cd}^{2+}$  concentration below 30 mg/l.

Analysis of the equilibrium data is important to develop an equation which accurately represents the results and can be used for the design purposes [31]. Several isotherm models have been used to describe the equilibrium between metal ions adsorbed onto the adsorbent and metal ions in the solution.

The Langmuir isotherm model assumes a monolayer adsorption onto a homogenous surface where the binding sites have equal affinity and energy, and no interaction between the adsorbed species [32]. The linear form of Langmuir isotherm equation is given by Eq. (3):

$$\frac{C_e}{q_e} = \frac{1}{K_L q_m} + \frac{C_e}{q_m} \quad (3)$$

Where  $q_e$  (mg/g) is the equilibrium concentrations of metal ions in the adsorbents,  $C_e$  (mg/l) is the equilibrium concentrations of metal ions in the liquid phases,  $q_m$  (mg/g) is the maximum adsorption amount representing monolayer coverage of adsorbent with adsorbate, and  $K_L$  (l/mg) is the Langmuir coefficient related to surface adsorption energy. A dimensionless constant  $R_L$ , which reflects the essential characteristic of Langmuir model, can be obtained as follows [33]:

$$R_L = \frac{1}{1 + K_L C_0} \quad (4)$$

Where  $C_0$  (mg/l) is the initial concentrations of metal ions in aqueous solution.

The Freundlich sorption isotherm model assumes that the adsorption of metal ions occurs on a heterogeneous surface by multilayer adsorption and that the amount of adsorbate adsorbed

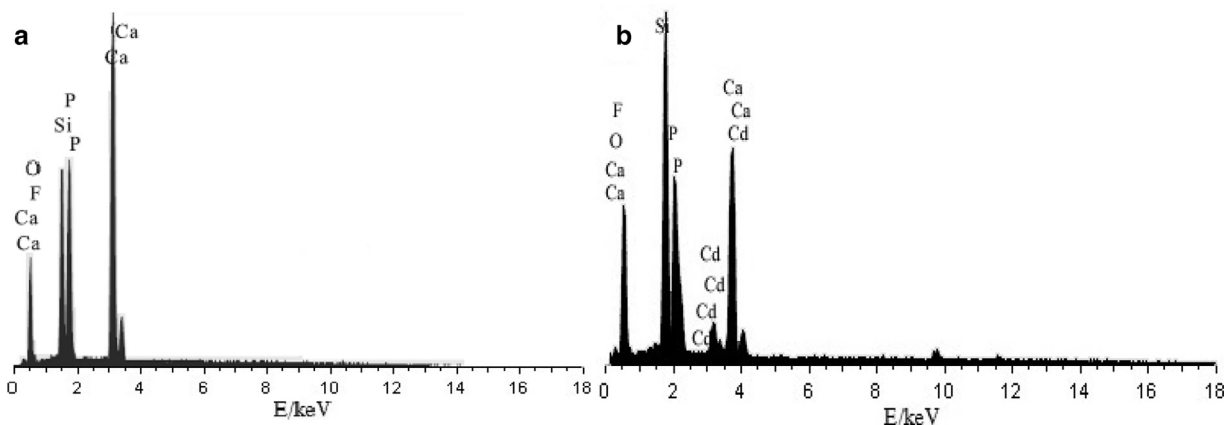


**Fig. 4.** EDS spectra of FHA (a) before and (b) after  $\text{Cd}^{2+}$  adsorption.

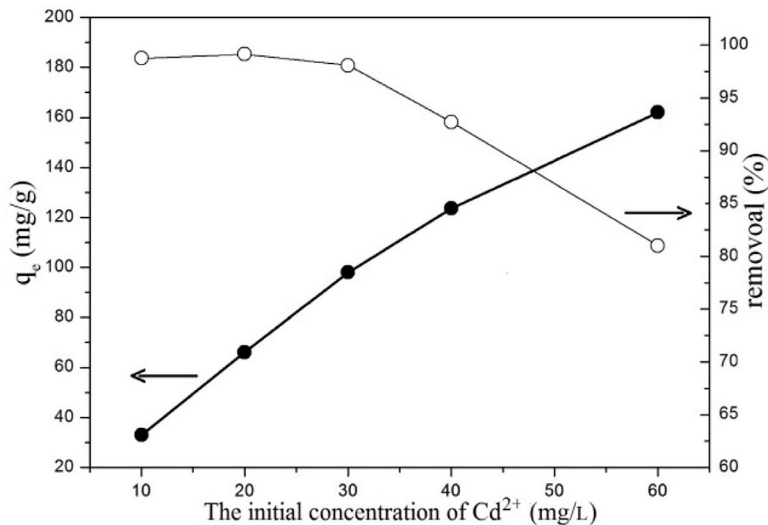


Fig. 5. The effect of initial  $\text{Cd}^{2+}$  concentration on the adsorption of FHA for  $\text{Cd}^{2+}$ . Amount of adsorbent FHA, 0.3 g/l; agitation speed, 130 r/min; solution pH, 7.0; adsorption time, 10 h; solution temperature, 25 °C.

Table 3

Langmuir, Freundlich and DKR parameters for adsorption of  $\text{Cd}^{2+}$  onto FHA at different temperatures.

$T/^\circ\text{C}$	Langmuir isotherm				Freundlich isotherm			DKR isotherm			Measured $q_e$ (mg/g)
	$R^2$	$q_m$ (mg/g)	$K_L$ (l/mg)	$R_L$	$R^2$	$K_f$ (mg/g)	$n^{-1}$	$R^2$	$q_m$ (mg/g)	$E$ (KJ/mol)	
15	0.9988	145.56	0.80	0.1114	0.9411	17.78	0.34	0.9949	168.99	7.91	137.16
25	0.9961	167.50	1.91	0.0255	0.8187	26.70	0.29	0.8705	141.97	9.13	162.03
35	0.9984	189.39	2.20	0.0149	0.8347	31.73	0.36	0.8854	270.25	8.45	177.89
45	0.9675	236.41	2.01	0.0082	0.9475	44.33	0.51	0.9606	408.85	7.91	193.84

increases infinitely with an increase in concentration [34,35]. The equilibrium data is correlated with the Freundlich isotherm by Eq. (5):

$$\ln q_e = \ln K_f + \frac{1}{n} \ln C_e \quad (5)$$

Where  $K_f$  is the Freundlich parameter related to the adsorption amount, and  $n$  is the Freundlich parameter related to the intensity of adsorption.

The Dubinin–Kaganer–Radushkevich (DKR) isotherm model has been used to describe the adsorption of metal ions on clays [34]. The DKR equation is expressed as follow [36]:

$$\ln q_e = \ln q_m - \beta [RT \ln(1 + 1/C_e)]^2 \quad (6)$$

Where  $\beta$  ( $\text{mol}^2/\text{J}^2$ ) is the activity coefficient related to mean adsorption energy,  $R$  (8.3145 J/(mol·K)) is the gas constant, and  $T$  (K) is the absolute temperature. Moreover, the constant  $\beta$  gives the mean free energy  $E$  (KJ/mol) of adsorption per molecule of the adsorbate for metal ions when it is transferred to the solid surface from bulk solution, and the adsorption energy can also be computed using the following relationship [37]:

$$E = \frac{1}{\sqrt{-2\beta}} \quad (7)$$

The Langmuir, Freundlich and DKR isotherm constants together with the correlation coefficients were presented in Table 3. From Table 3, the  $R_L$  values for the Langmuir model were all smaller than 1.0 suggesting it was a favorable adsorption of FHA for  $\text{Cd}^{2+}$  in aqueous solution. Furthermore, the correlation coefficients ( $R^2 > 0.96$ ) for Langmuir isotherm model was found good agreement between theoretical model and experimental results in this

work better than the Freundlich isotherm model ( $R^2 > 0.81$ ) and DKR isotherm model ( $R^2 > 0.87$ ), indicating that the adsorption of  $\text{Cd}^{2+}$  on FHA was well described by the Langmuir isotherm. The reason could be attributed to the homogeneous nature of active sites on the surface of FHA, and a monolayer adsorption occurred between FHA and  $\text{Cd}^{2+}$ . The Langmuir constant  $K_L$  increased with the increasing adsorption temperature suggesting that adsorption amount of  $\text{Cd}^{2+}$  was proportional to the temperature, which was further evidenced by the maximum adsorption amount,  $q_m$ , value was 236.41 mg/g at temperature of 45 °C. And the phenomenon appeared may be due to the decreasing of the activation energy for  $\text{Cd}^{2+}$  on FHA and the affinity of adsorption sites increasing as the temperature increased, which would be further investigated in a follow-up experiment. However, the correlation coefficients for the Freundlich and DKR isotherm models were favorably at a certain temperature, demonstrating that the adsorption of  $\text{Cd}^{2+}$  on FHA could be described by these models partially. The numerical value of  $n^{-1}$  (0.2–0.5) from Freundlich isotherm model demonstrated that adsorption capacity was only slightly decreased at lower equilibrium concentrations [38], and the isotherm did not predict any saturation of the sorbent by the sorbate, thus infinite surface coverage was predicted mathematically, indicating that multilayer adsorption on the surface. And the adsorption energy  $E$  (7.91–9.13 KJ/mol) from DKR isotherm model was calculated that the adsorption type could be explained by physical adsorption and ion-exchange.

The comparison of the maximum adsorption amount for  $\text{Cd}^{2+}$  on different adsorbents was summarized in Table 4. Although direct comparison of FHA with other adsorbent materials was difficult, owing to the differences in experimental conditions, it was found that the maximum adsorption amount of FHA was higher

**Table 4**  
Comparison of Cd<sup>2+</sup> adsorption onto FHA with other adsorbents.

Adsorbents	q <sub>e</sub> (mg/g)	Reference
Apatite II™ derived from fish bones	92.00	[8]
Moroccan stevensite	22.37 <sup>a</sup>	[37]
Impregnated Styrofoam	29.11	[38]
Melamine-formaldehyde-DTPA chelating resin	102.51	[39]
Poly (vinyl alcohol)/chitosan	126.06	[40]
Chitosan crosslinked with epichlorohydrin-triphosphate	83.75 <sup>a</sup>	[41]
PVA-immobilized <i>Aspergillus niger</i>	60.24	[42]
Kraft lignin	137.14	[43]
Black gram husk	39.99	[44]
Activated carbon (Filtrisorb)	307.50	[45]
One char	64.07	[46]
Nano-hydroxyapatite by microwave heating (H <sub>3</sub> PO <sub>4</sub> , Ca(NO <sub>3</sub> ) <sub>2</sub> ·4H <sub>2</sub> O)	88.50	[1]
nHAP purchased from Anpuruinano material company (Nanjing, China)	64.07	[2]
Magnetic hydroxyapatite nanoparticles	127.80	[14]
Nano crystallite hydroxyapatite	142.86	[34]
Novel biopolymer-coated hydroxyapatite foams	35.52	[47]
Flour-hydroxyapatite composites	193.84	Present work

<sup>a</sup> The Langmuir maximum amount.

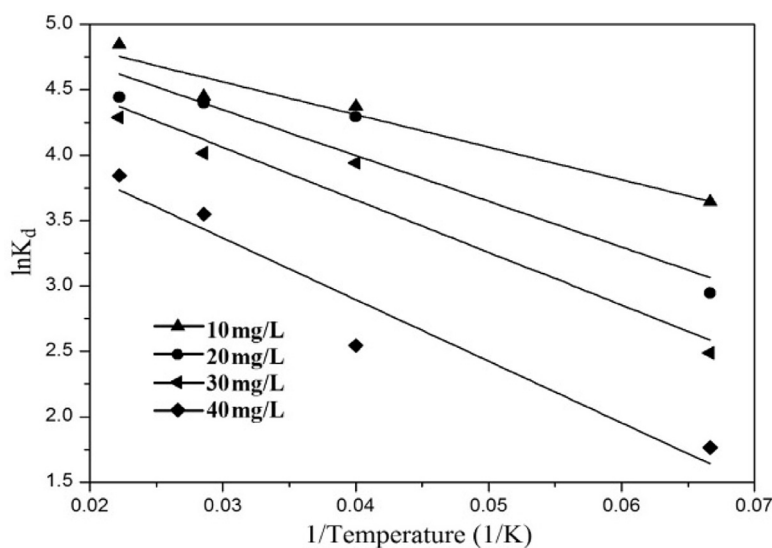


**Fig. 6.** Linear fit of experimental data obtained by plotting of  $\ln K_d$  versus  $1/T$  for Cd<sup>2+</sup> adsorption onto FHA at different initial Cd<sup>2+</sup> concentrations. Amount of adsorbent FHA, 0.3 g/l; agitation speed, 130 r/min; solution pH, 7.0; adsorption time, 10 h.

than most adsorbents presented in Table 4. Therefore, it could be concluded that FHA had a considerable potential advantage for the removal of Cd<sup>2+</sup> from aqueous solution.

### 3.4. Effect of temperature and adsorption thermodynamics

The effect of temperature on the adsorption of Cd<sup>2+</sup> onto FHA from Table 3 showed that the adsorption amount increased as the temperature increased, suggesting that the adsorption process was endothermic in nature [28].

Thermodynamic parameters ( $\Delta G^0$ ,  $\Delta H^0$  and  $\Delta S^0$ ) are calculated by Van't Hoff equation:

$$\ln K_d = \frac{\Delta S^0}{R} - \frac{\Delta H^0}{RT} \quad (8)$$

$$\Delta G^0 = -RT \ln K_d \quad (9)$$

The linear fit of thermodynamics for the adsorption process was shown in Fig. 6 and the thermodynamic parameters were given in Table 5. The enthalpy change  $\Delta H^0 > 0.21$  kJ/mol indicated the endothermic nature of the adsorption for Cd<sup>2+</sup>. The Gibbs free energy

$\Delta G^0 < -1.38$  kJ/mol at various temperature indicated the feasibility of the process and spontaneous nature of the adsorption. Furthermore, the  $\Delta G^0$  values decreased with an increase in temperature, suggesting an increased trend in the degree of spontaneity and feasibility of Cd<sup>2+</sup> adsorption. The values of  $\Delta S^0 > 39.74$  kJ/mol suggested that the degree of freedom increased at the solid-liquid interface during the adsorption. The reason for this phenomenon was that the surface of FHA existed enough adsorption sites which were activated to complex Cd<sup>2+</sup> in solution with increase in temperature, and the activation energy of adsorption for Cd<sup>2+</sup> was decreased, resulting in the increased affinity of the FHA for Cd<sup>2+</sup> and the randomness in the adsorbent-pollutant system [39].

### 3.5. Effect of contact time and adsorption kinetics

The effect of contact time on the adsorption of Cd<sup>2+</sup> onto FHA was shown in Fig. 7 and the adsorption kinetics was established. It was found that the amount of Cd<sup>2+</sup> adsorbed onto FHA increased with an increase in contact time, and higher removal efficiencies were obtained in 15 min. Moreover, the initial Cd<sup>2+</sup> concentration had an evident effect on the adsorption process to reach the equilibrium. The time needed for the initial Cd<sup>2+</sup>

**Table 5**  
Thermodynamics parameters for Cd<sup>2+</sup> adsorption onto FHA at different initial Cd<sup>2+</sup> concentrations.

Concentration of Cd <sup>2+</sup> (mg/l)	$\Delta G^0$ (KJ/mol)				$\Delta H^0$ (KJ/mol)	$\Delta S^0$ (J/(mol·K))
	288 K	298 K	308 K	318 K		
10	-3.0962	-3.6547	-3.8228	-4.1725	0.2074	44.1467
20	-2.5871	-3.6111	-3.7931	-3.9428	0.2852	44.8858
30	-2.1823	-3.3975	-3.5610	-3.8503	0.3355	43.7850
40	-1.3815	-2.3137	-3.2436	-3.5609	0.3915	39.7367

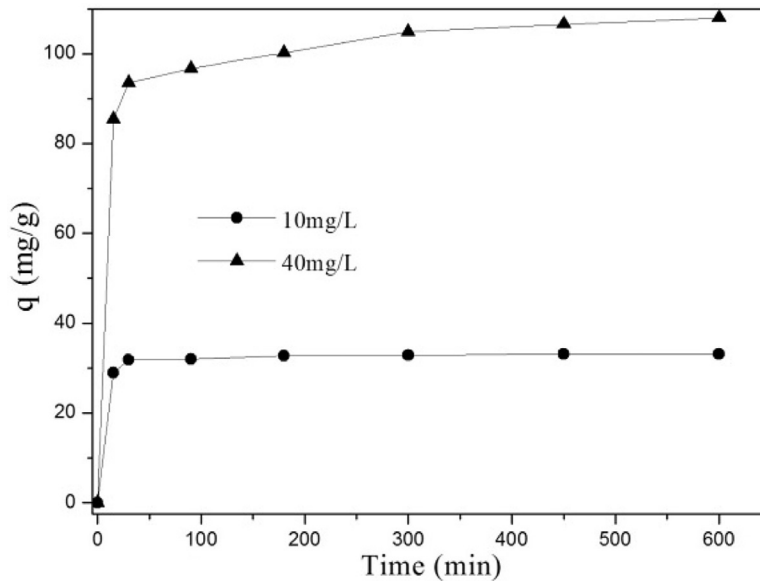


**Fig. 7.** The effect of contact time on the adsorption of Cd<sup>2+</sup> onto FHA. Amount of adsorbent FHA, 0.3 g/l; agitation speed, 130 r/min; solution pH, 5.0; solution temperature, 25 °C.

**Table 6**  
Kinetic parameters for Cd<sup>2+</sup> adsorption onto FHA at different initial Cd<sup>2+</sup> concentrations.

Concentration (mg/l)	Pseudo-first-order kinetic			Pseudo-second-order kinetic				Measured $q_e$ (mg/g)
	$q_e$ (mg/g)	$K_1$ (1/min)	$R_1^2$	$q_e$ (mg/g)	$K_2$ (g/(mg·min))	$h$ (mg/(g·min))	$R_2^2$	
10	2.56	0.0063	0.6751	19.96	0.0389	15.50	1.0000	19.8858
40	18.63	0.0056	0.8306	65.36	0.0035	14.95	0.9996	67.6000

concentration of 10 mg/l to reach the equilibrium was 30 min, while it took about 300 min for initial Cd<sup>2+</sup> concentration of 40 mg/l. Therefore, the time needed for various initial Cd<sup>2+</sup> concentrations was chosen for 10 h to reach the adsorption equilibrium.

In spite of many mathematical models were proposed to interpret the transport of solutes inside adsorbent, the complexity of mathematical models made them inconvenient in practice [48]. The rate models generally evaluated by the pseudo-first-order (Eq. (10)) and pseudo-second-order (Eq. (11)) [49]:

$$\ln(q_e - q_t) = \ln q_e - K_1 t \quad (10)$$

$$\frac{t}{q_t} = \frac{1}{K_2 q_e^2} + \frac{t}{q_e} \quad (11)$$

Where  $q_e$  (mg/g) is the amount of Cd<sup>2+</sup> adsorbed onto FHA at equilibrium,  $q_t$  (mg/g) is the amount of Cd<sup>2+</sup> adsorbed onto FHA at time  $t$  (min),  $K_1$  (min<sup>-1</sup>) is the constant of the pseudo-first-order equation, and  $K_2$  (g/(mg·min)) is the constant of the pseudo-second-order equation. Additionally,  $h$  (mg/(g·min)) is the initial adsorption rate of pseudo-second-order kinetic model which can be calculated using  $h = K_2 q_e^2$ .

The kinetic models were applied to fitting experimental data, the results were presented in Fig. 8 and Table 6. Based on Fig. 8 and Table 6, the pseudo-second-order kinetic model provided preferable match between theoretical and experimental  $q_e$  values, and showed a better correlation for experimental data. These results indicated that the chemisorption involving valence forces through the sharing or exchange of electrons between adsorbent and metal ions is rate-limiting step in adsorption process of FHA for Cd<sup>2+</sup> [50–52]. The calculated  $h$  and  $K_2$  values were higher at low initial Cd<sup>2+</sup> concentration, suggesting that the adsorption process was much faster at low initial Cd<sup>2+</sup> concentration.

### 3.6. Desorption experiment

In order to investigate the potential of FHA for real application, desorption of the adsorbed Cd<sup>2+</sup> from adsorbent was studied by the batch method using different kinds of eluents including HAC, Ca(NO<sub>3</sub>)<sub>2</sub>, EDTA-2Na and NaOH. The efficiencies of different eluents to release Cd<sup>2+</sup> from loaded FHA were shown in Table 7. It was observed that the highest desorption value for Cd<sup>2+</sup> (45.09%) was obtained using HAC solution, while the amount desorbed from the NaOH solution was the lowest. This phenomenon could be explained that FHA existed stably in alkaline solution rather than in

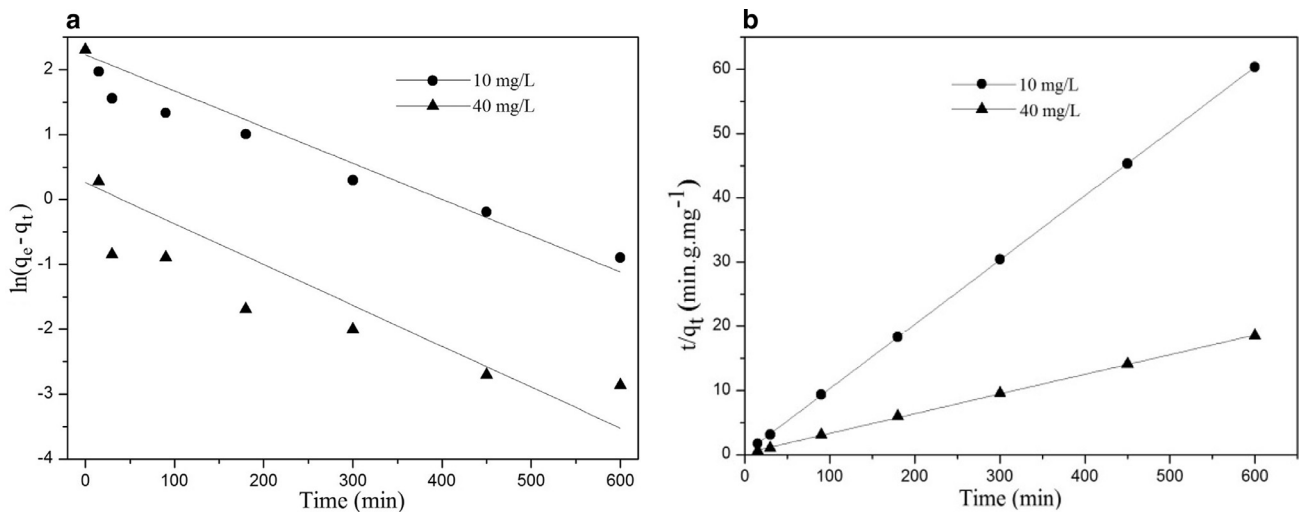


**Fig. 8.** The linearized pseudo-first/second-order kinetic plots for  $\text{Cd}^{2+}$  adsorption under different initial concentrations. Amount of adsorbent FHA, 0.3 g/l; agitation speed, 130 r/min; solution pH, 5.0; solution temperature, 25 °C.

**Table 7**

Desorption of  $\text{Cd}^{2+}$  from loaded FHA adsorbents.

Eluents	Initial pH	Final pH	Desorbed (%)
HAc (0.01 mol/l)	3.34	3.67	45.09
$\text{Ca}(\text{NO}_3)_2$ (0.01 mol/l)	5.95	6.01	31.24
EDTA-2Na (0.01 mol/l)	4.57	4.36	6.63
NaOH (0.01 mol/l)	11.88	11.51	1.43

acidic solution. Furthermore, the favorable amount of  $\text{Cd}^{2+}$  desorbed in the  $\text{Ca}(\text{NO}_3)_2$  solution was 31.24% due to the reversible process of cationic exchange between the FHA adsorbents surface and the solution [11].

#### 4. Conclusions

The economic adsorbent FHA based on fluorine-contained silica (F-SiO<sub>2</sub>) from fluorine industry was prepared, characterized and used for the removal of  $\text{Cd}^{2+}$  from aqueous solution, which eliminated the fluoride pollution and changed waste into valuable. FHA with rod-like and developed space connected structure exhibited good mass transfer property, excellent adsorbability and fast kinetics for  $\text{Cd}^{2+}$  in aqueous solution. Some factors affecting the adsorption process such as solution pH, initial  $\text{Cd}^{2+}$  concentration, contact time and temperature were studied. The equilibrium data of  $\text{Cd}^{2+}$  were best fitted the Langmuir isotherm, and the adsorption kinetics followed the pseudo-second-order kinetic model. According to the results of effects of pH, adsorption isotherms and kinetics, the adsorption mechanisms of FHA were mainly determined by ion-exchange and monolayer chemical adsorption. Besides, the thermodynamic parameters depicted the endothermic nature of adsorption and the process was spontaneous. Desorption experiments indicated the most efficient eluent used for desorption of  $\text{Cd}^{2+}$  was HAc with more than 45% of  $\text{Cd}^{2+}$  released. In this work, FHA provided a potential application in the treatment of wastewater because of its excellent adsorption performance.

#### Acknowledgments

This work was supported by the Phosphorus Key Technology R&D Program of Sichuan University (SCU2015C002); and the Applied Basic Research Programs of Science and Technology Commis-

sion Foundation of Sichuan Province (No. 2014JY0079), the People's Republic of China.

#### References

- [1] Elkady MF, Mahmoud MM, Abd-El-Rahman HM. Kinetic approach for cadmium sorption using microwave synthesized nano-hydroxyapatite. *J Non-Cryst Solids* 2011;357:1118–29.
- [2] Zhang ZZ, Li MY, Chen W, Zhu SZ, Liu NN, Zhu LY. Immobilization of lead and cadmium from aqueous solution and contaminated sediment using nano-hydroxyapatite. *Environ Pollut* 2010;158:514–19.
- [3] Bhatluri KK, Manna MS, Ghoshal AK, Saha P. Supported liquid membrane based removal of lead(II) and cadmium(II) from mixed feed: conversion to solid waste by precipitation. *J Hazard Mater* 2015;299:504–12.
- [4] Hizal J, Apak R. Modeling of cadmium(II) adsorption on kaolinite-based clays in the absence and presence of humic acid. *Appl Clay Sci* 2006;32:232–44.
- [5] Wei W, Bediako JK, Kim S, Yun YS. Removal of Cd(II) by poly(styrenesulfonic acid)-impregnated alginate capsule. *J Taiwan Inst Chem E* 2016;61:188–95.
- [6] Cui Y, Ge QC, Liu XY, Chung TS. Novel forward osmosis process to effectively remove heavy metal ions. *J Membrane Sci* 2014;467:188–94.
- [7] Boschi C, Maldonado H, Ly M, Guibal E. Cd(II) biosorption using *Lessonia* kelps. *J Colloid Interf Sci* 2011;357:487–96.
- [8] Oliva J, Pablo JD, Cortina JL, Cama J, Ayora C. Removal of cadmium, copper, nickel, cobalt and mercury from water by apatite II<sup>TM</sup>: Column experiments. *J Hazard Mater* 2011;194:312–23.
- [9] Crini G. Recent developments in polysaccharide-based materials used as adsorbents in wastewater treatment. *Prog Polym Sci* 2005;30:38–70.
- [10] Corami A, Mignardi S, Ferrini V. Cadmium removal from single- and multi-metal(Cd+Pb+Zn+Cu) solutions by sorption on hydroxyapatite. *J Colloid Interf Sci* 2008;317:402–8.
- [11] Simon FG, Biermann V, Peplinski B. Uranium removal from groundwater using hydroxyapatite. *Appl Geochem* 2008;23:2137–45.
- [12] Sundaram CS, Viswanathan N, Meenakshi S. Defluoridation chemistry of synthetic hydroxyapatite at nano scale: equilibrium and kinetic studies. *J Hazard Mater* 2008;155:206–15.
- [13] Krestou A, Xenidis A, Panias D. Mechanism of aqueous uranium(VI) uptake by hydroxyapatite. *Miner Eng* 2004;17:373–81.
- [14] Feng Y, Gong JL, Zeng GM, Niu QY, Zhang HY, Niu CG, et al. Adsorption of Cd(II) and Zn(II) from aqueous solutions using magnetic hydroxyapatite nanoparticles as adsorbents. *Chem Eng J* 2010;162:487–94.
- [15] Gómez del Río J, Sanchez P, Morando PJ, Cicerone DS. Retention of Cd, Zn and Co on hydroxyapatite filters. *Chemosphere* 2006;64:1015–20.
- [16] Corami A, Mignardi S, Ferrini V. Copper and zinc decontamination from single- and binary-metal solutions using hydroxyapatite. *J Hazard Mater* 2007;146:164–70.
- [17] Aliabadi M, Irani M, Ismaeili J, Najafzadeh S. Design and evaluation of chitosan/hydroxyapatite composite nanofiber membrane for the removal of heavy metal ions from aqueous solution. *J Taiwan Inst Chem E* 2014;45:518–26.
- [18] Hokkanen S, Bhatnagar A, Repo E, Lou S, Sillanpää M. Calcium hydroxyapatite microfibrillated cellulose composite as a potential adsorbent for the removal of Cr(VI) from aqueous solution. *Chem Eng J* 2016;283:445–52.
- [19] Wakamura M, Kandori K, Ishikawa T. Surface composition of calcium hydroxyapatite modified with metal ions. *Colloid Surface A* 1998;142:107–16.
- [20] Kousalya GN, Gandhi MR, Sundaram CS, Meenakshi S. Synthesis of nano-hydroxyapatite chitin/chitosan hybrid biocomposites for the removal of Fe(III). *Carbohydr Polym* 2010;82:594–9.

- [21] Islam M, Mishra PC, Patel R. Arsenate removal from aqueous solution by cellulose-carbonated hydroxyapatite nanocomposites. *J Hazard Mater* 2011;189:755–63.
- [22] Jiménez-Reyes M, Solache-Ríos M. Sorption behavior of fluoride ions from aqueous solutions by hydroxyapatite. *J Hazard Mater* 2010;180:297–302.
- [23] Huang CP, Wang J, Che DC. Study of the crystal structures of the fluoridated apatite coatings electrodeposited on titanium. *Rare Metal Mat Eng* 2011;40:233–6.
- [24] Wen XD, Deng QW, Guo J, Yang SC. Ultra-sensitive determination of cadmium in rice and water by UV-vis spectrophotometry after single drop microextraction. *Spectrochim Acta A* 2011;79:508–12.
- [25] Singh AK, Ratnam BK. Spectrophotometric determination of cadmium with dithizone in water analysis – improvement in sensitivity by surfactant-induced sensitization. *Microchem J* 1989;39:241–3.
- [26] Zhu XH, Zhang Z, Shen J. Kinetics and mechanism of adsorption of phosphate on fluorine-containing calcium silicate. *J Wuhan Univ Technol* 2016;31:321–7.
- [27] Zhu RH, Yu RB, Yao JX, Mao D, Xing CJ, Wang D. Removal of Cd<sup>2+</sup> from aqueous solutions by hydroxyapatite. *Catal Today* 2008;139:94–9.
- [28] Li XL, Li YF, Zhang SD, Ye ZF. Preparation and characterization of new foam adsorbents of poly(vinyl alcohol)/chitosan composites and their removal for dye and heavy metal from aqueous solution. *Chem Eng J* 2012;183:88–97.
- [29] Wu LM, Forsling W, Schindler PW. Surface complexation of calcium minerals in aqueous solution: 1. Surface protonation at fluorapatite–water interfaces. *J Colloid Interf Sci* 1991;147:178–85.
- [30] Smičiklas I, Dimović S, Plečaš I, Mitrić M. Removal of Co<sup>2+</sup> from aqueous solutions by hydroxyapatite. *Water Res* 2006;40:2267–74.
- [31] Aksu Z. Determination of the equilibrium, kinetic and thermodynamic parameters of the batch biosorption of nickel(II) ions onto *Chlorella vulgaris*. *Process Biochem* 2002;38:89–99.
- [32] Langmuir I. The adsorption of gases on plane surfaces of glass, mica and platinum. *J Am Chem Soc* 1918;40:1361–403.
- [33] Gupta VK, Ali I. Removal of lead and chromium from wastewater using bagasse fly ash–a sugar industry waste. *J Colloid Interf Sci* 2004;271:321–8.
- [34] Mobasherpour I, Salahi E, Pazouki M. Removal of divalent cadmium cations by means of synthetic nano crystallite hydroxyapatite. *Desalination* 2011;266:142–8.
- [35] Freundlich HMF. Über die adsorption in lösungen. *Z Phys Chem-Leipzig* 1906;57:385–470.
- [36] Dubinin MM, Radushkevich LV. Equation of the characteristic curve of activated charcoal. *Chem Zentr* 1947;1:875–90.
- [37] Benhammou A, Yaacoubi A, Nibou L, Tanouti B. Adsorption of metal ions onto Moroccan stevensite: kinetic and isotherm studies. *J Colloid Interf Sci* 2005;282:320–6.
- [38] Memon SQ, Bhangar MI, Hasany SM, Khuhawar MY. Sorption behavior of impregnated Styrofoam for the removal of Cd(II) ions. *Colloid Surface A* 2006;279:142–8.
- [39] Baraka A, Hall PJ, Heslop MJ. Preparation and characterization of melamine-formaldehyde-DTPA chelating resin and its use as an adsorbent for heavy metals removal from wastewater. *React Funct Polym* 2007;67:585–600.
- [40] Li XL, Li YF, Ye ZF. Preparation of macroporous bead adsorbents based on poly(vinyl alcohol)/chitosan and their adsorption properties for heavy metals from aqueous solution. *Chem Eng J* 2011;178:60–8.
- [41] Laus R, Costa TG, Szpoganicz B, Fávère VT. Adsorption and desorption of Cu(II), Cd(II) and Pb(II) ions using chitosan crosslinked with epichlorohydrin-triophosphate as the adsorbent. *J Hazard Mater* 2010;183:233–41.
- [42] Tsekova K, Todorova D, Dencheva V, Ganeva S. Biosorption of copper(II) and cadmium(II) from aqueous solutions by free and immobilized biomass of *Aspergillus niger*. *Bioresource Technol* 2010;101:1727–31.
- [43] Mohan D, Pittman Jr CU, Steele PH. Single, binary and multi-component adsorption of copper and cadmium from aqueous solutions on Kraft lignin–a biosorbent. *J Colloid Interf Sci* 2006;297:489–504.
- [44] Saeed A, Iqbal M, Akhtar MW. Removal and recovery of lead(II) from single and multimetal (Cd, Cu, Ni, Zn) solutions by crop milling waste (black gram husk). *J Hazard Mater* 2005;117:65–73.
- [45] Kapoor A, Viraraghavan T, Cullimore DR. Removal of heavy metals using the fungus *Aspergillus niger*. *Bioresource Technol* 1999;70:95–104.
- [46] Cheung CW, Porter JF, Mckay G. Sorption kinetic analysis for the removal of cadmium ions from effluents using bone char. *Water Res* 2001;35:605–12.
- [47] Vila M, Sánchez-Salcedo S, Cicuéndez M, Izquierdo-Barba I, Vallet-Regí M. Novel biopolymer-coated hydroxyapatite foams for removing heavy-metals from polluted water. *J Hazard Mater* 2011;192:71–7.
- [48] Biswas BK, Inoue K, Ghimire KN, Ohta S, Harada H, Ohto K, et al. The adsorption of phosphate from an aquatic environment using metal-loaded orange waste. *J colloid interf Sci* 2007;312:214–23.
- [49] Ho YS, Mckay G. A comparison of chemisorption kinetic models applied to pollutant removal on various sorbents. *Process Saf Environ* 1998;76:332–40.
- [50] Uzun I, Güzel F. Rate studies on the adsorption of some dyestuffs and p-nitrophenol by chitosan and monocarboxymethylated(mcm)-chitosan from aqueous solution. *J Hazard Mater* 2005;118:141–54.
- [51] Chiou MS, Li HY. Adsorption behavior of reactive dye in aqueous solution on chemical cross-linked chitosan beads. *Chemosphere* 2003;50:1095–105.
- [52] Hu XJ, Wang JS, Liu YG, Li X, Zeng GM, Bao ZL, et al. Adsorption of chromium(VI) by ethylenediamine-modified cross-linked magnetic chitosan resin: isotherms, kinetics and thermodynamics. *J Hazard Mater* 2011;185:306–14.